9th International Conference on Fibre-Reinforced Polymer (FRP) Composites in Civil Engineering (CICE 2018), PARIS 17-19 JULY 2018

COMPRESSIVE BEHAVIOR OF CONCRETE COLUMNS AXIALLY-LOADED BEFORE CFRP-WRAPPING. REMARKS BY EXPERIMENTAL-NUMERICAL INVESTIGATION

M.F. Ferrotto[1,2], O. Fischer[3], R. Niedermeier[3], L. Cavaleri[2]
[1] *University of Palermo, Italy, Email: marcofilippo.ferrotto@unipa.it*
[2] *University of Palermo, Department of Civil, Environmental, Aerospace, Materials Engineerng, Italy*
[3] *Technical University of Munich (TUM), Department of Civil, Geo and Environmental Engineering, Germany.*

ABSTRACT

Strengthening of existing concrete columns with Fiber Reinforced Polymers (FRP) results generally in a satisfactory structural member improvement in terms of load and strain capacity. A reliable prediction of the capacity obtained by these reinforcement strategies requests a proper knowledge of the load-strain response of the confined concrete elements. However, so far, the available design methods and technical codes do not consider the effect of the possible presence of service loads at the moment of application of the reinforcement, and therefore, the compressive behavior of the concrete confined under preload is still unclear.
In this paper, the effect of sustained loads on the compressive behavior of concrete columns CFRP-confined while preloaded is analyzed. Experimental tests were performed on circular concrete columns confined under low, medium and high preload levels before wrapping ad subsequently loaded until failure, observing the differences respect to the standard compressive stress-strain response of FRP-confined concrete. A finite element (FE) model is also developed by using ABAQUS software to simulate the physical scheme of the experimental tests. The accuracy of the model is validated through comparing with the experimental results.

KEYWORDS

Preloading, FRP-confined concrete, axial compressive behavior, finite element modeling.

INTRODUCTION

In the last decades, several authors have focused on an evaluation of the confinement capacity of reinforced columns with no stress/strain at the time of application of the FRP wraps (Spoelstra and Monti 1999, Lam and Teng 2004, Teng et al. 2007). However, very few resources are available regarding existing stress/strain (i.e. preloading) and the respective effect on the bearing and deformational capacity of the columns after wrapping. In fact, this aspect, which could significantly change the performance of reinforced members, is still unclear. This lack of understanding is due to the difficulty of performing realistic tests and numerical-analytical approaches suffering in terms of reliability because of the limited number of available experimental data.
Only few studies can be found in literature not always leading to the same conclusions. Some authors state that the effect of sustained loads is not particularly influent on the load-bearing capacity of the FRP-confined members (Shi and He 2009), others state that the pre-existing loads are positive for low preload levels and negative for high preload levels (He and Jin 2011), others assess that the preload affects negatively the response in compression of a FRP-wrapped member, reducing the strength and the corresponding strain of the confined concrete (Pan et al. 2016). All these different statements certainly entail confusion for the practical application when instead it would be important to have a solid basis and adequate design recommendations.
The basic problem lies in the evaluation of the compressive behavior of columns that are subjected to external confinement while preloaded, observing how the subsequent increasing of load could change the compressive response of the columns respect to the standard compressive response (with no preload).
In the present paper, the issue is analyzed firstly by experimental investigation carried out on medium-scale concrete columns subjected to a certain axial load, wrapped with FRP jackets and subsequently loaded until failure. The stress-strain response of columns with preload was compared with that provided by the same FRP-wrapped columns subjected to monotonic compressive loads according to the classical compression tests. The physical scheme of the experimental tests was then reproduced by means of finite element modeling technique associated with the advanced technique of modeling with deactivation/reactivation elements available in the Abaqus software package.

EXPERIMENTAL INVESTIGATION

Specimens preparation and test setup

Compression tests were carried out on nineteen circular plain concrete specimens with diameter of 150 mm and height of 600 mm, having compressive strength of 38.13 MPa and 41.7 MPa for concrete type A and type B respectively. The tests were summarized into three categories, namely compression tests on unconfined cylinders, compression tests on confined cylinders and compression tests with preload.

The preload level index was defined as the ratio of the preloading force applied to the specimens before wrapping (P or $\sigma_{(\varepsilon)}$) and the ultimate unconfined axial load/strength capacity (P_{max} or f_{c0}).

$$n_p = \frac{P}{P_{\max}} = \frac{\sigma_{(\varepsilon)}}{f_{c0}} \qquad 0 \le n_p \le 1 \tag{1}$$

Strengthening of the specimens was made by unidirectional carbon fiber textile having nominal thickness t_f equal to 0.131 mm (based on the total area of the carbon fibers), nominal tensile strength of the fibers f_{ju} equal to 4300 MPa, elastic modulus E_j of 234 GPa and ultimate strain ε_{ju} of 1.8%. Epoxy resin for the CFRP consisted of two components, which are the main component and the hardener. The mixing ratio by weight was 4:1 based on the provisions of the technical sheet. The specimens were confined with three and two Carbon FRP layers for concrete type A and type B respectively.

The tests were carried out using calibrated compression testing machines with nominal maximum loading capacities of 5 MN and 10 MN, displacement controlled by a servo-hydraulic management system electronically controlled through a computer interface. During the preloading and the failure test, the load was applied displacement controlled with a deformation rate of 0.2 mm/(m·min).

Regarding the tests on preloaded specimens, the concrete cylinders were placed into a specially designed frame system, consisting of two triangular steel plates with drilled holes in which threaded steel bars were inserted having the function - as a result of the screwing of the nuts and loading the disc springs positioned at the ends of the bars - to keep constant and to center the compression load (Figure 1). By means of a load cell, placed between the bottom plate and the specimens, the load was monitored and subsequently correlated with the corresponding deformations of the concrete obtained by reading of horizontal and vertical strain gauges.

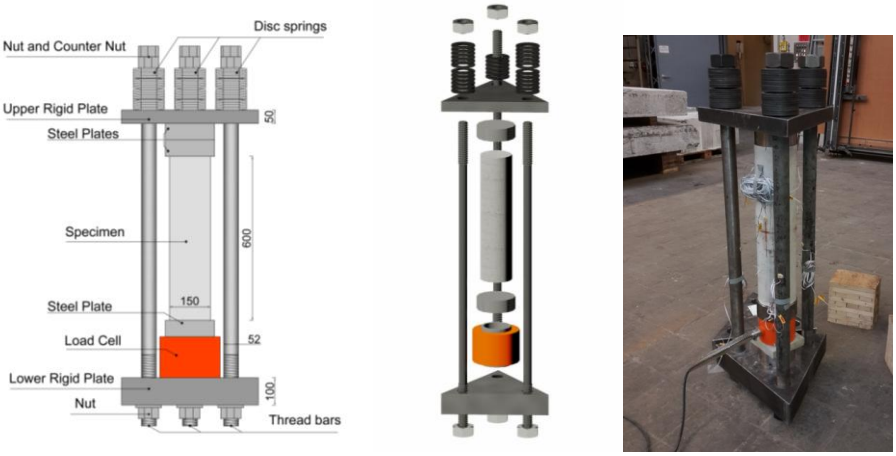

(a) Frame system details *(b) Assembling* *(c) Real view*

Figure 1: Test frame system for preloaded specimens

The load was transmitted from the machine to the specimen by applying a uniform compression load on adequately designed non-linear disc springs. When the preloading target level was reached, the screwing of the nuts on the threaded bars began up to the unloading of the machine so that, at the end of the preloading test, compression load on the specimens was provided only from the bars.

The strengthening of the preloaded specimens was made in presence of a certain compression stress. To ensure a limited loss of load due to creep effects on the concrete during the curing process of the epoxy resin, the disc springs were arranged in such way that the shortening of the concrete cylinders was compensated by the travel of the springs.

After the curing process the specimens were placed into the load testing machine to perform the failure test. The load was applied directly to the specimens by means of steel plates placed in contact between the upper steel plate of the test frame and the upper steel plate of the testing machine. Arrangement of the test scheme for the preloading and the failure test is reported in Figure 2.

(a) Preloading of a specimen *(b) Wrapping under load* *(c) Compressive failure test*

Figure 2:Test sequence for specimens with preload

Preloading tests

Three different preloading levels (lower, medium and high) to observe differences respect to the reference specimens without preload were provided. For the concrete type A preloading levels of about 40%, 60% and 80% of f_{c0}, while for the concrete type B, preloading levels of about 55%, 70% and 90% of f_{cm} were applied before wrapping the specimens.

Specimens were classified by a label in function of the concrete type and the preloading level: the first letter of this label indicates the concrete type (A or B), the second letter indicates the types of test (S to indicate strengthened specimens without preloading, P preloaded specimen), the following number indicates the preloading level and the last number identifies the number of the specimen of the same category (Table 1). To provide an example, specimen AP80-1 indicates specimens with concrete type A, preloaded up to 80% of the strength of the unconfined concrete, strengthened with 3 carbon fibers sheets. For more details, please refer to Ferrotto et al. (2017).

Table 1: Classification of the specimens and preload levels

Specimens	f_{c0} (MPa)	ρ=4t/D	np (%)	Preload force (kN)
A1	38.13	/	/	/
AS1		0.0105	/	/
AS2			/	/
AS3			/	/
AP40-1			39	292
AP40-2			39	292
AP60-1			58.4	393
AP60-2			58.4	393
AP80-1			78	525
AP80-2			78	525
B1	41.7	/	/	/
BS1		0.007	/	/
BS2			/	/
BP55-1			55	393
BP55-2			55	393
BP70-1			71	525
BP70-2			71	525
BP90-1			88.5	655
BP90-2			88.5	655

For the specimens subjected to lower and medium preload levels (as specimens AP40-1, AP40-2, BP55-1 and BP55-2) after the achievement of the target preload a very stable behavior was found respect to the cylinders subjected to high preloading levels. No damage was observed for the plain concrete and the loss of load due to the creep and relaxation effects was negligible (for the preloaded specimens up to the 55% of the unconfined concrete strength the loss of load was lower than 7%).

Under high preloading conditions (between 55% and 90%) slightly more unstable behavior was observed: for the specimens AP80-1, AP80-2, BP90-1 and BP90-2, micro-cracks occurred in the plain concrete and nonlinear behavior of concrete resulted in a slightly higher loss of load during the subsequent steps. Despite this, in the worst cases the loss of load did not exceed 18%.

Failure tests

Concrete compression crushing failure was observed for the specimens without FRP wraps (A1 and B1) with smeared vertical cracking formed near to the crushing load (about 90% of the compressions strength of the material). The very good compaction of the concrete during the casting process provided to the specimens a good compression behavior so that cracking resulted as much as possible reduced and near to the failure conditions. This aspect was utmost of importance for the tests with preload because the absence of cracks avoided stress concentration of tension on the fibers without causing premature failure of the confined specimens.
The analysis of the results obtained from tests with preload allowed to state that the ultimate capacity of the confined specimens seems to be not particularly affected by the preloading level reached before applying the CFRP sheets. All the tested specimens showed similar behavior at failure characterized by the achievement of the rupture strain of the carbon fibers (Figure 3) and a comparable ultimate load. Instead, a difference between the two types of test was observed in the load-strain behavior in terms of reduction of the secant stiffness (slight decrease in slope with increasing of the preload levels). This reduction was due to the strain-lag of the composite jacket that causes, for same values of lateral strain of the concrete, lower values of lateral pressure.

(a) Specimens with no preload *(b) Preloaded specimens*

Figure 3: Specimens at collapse

FINITE ELEMENT MODELING

The concrete cylinder was modeled with C3D8R elements (8-node linear brick, reduced integration, hourglass control). Boundary conditions were defined assigning displacement and encastre to reference points of rigid bodies at the top and the bottom of the cylinder respectively. FRP sheet was modeled utilizing S4R elements (a 4-node doubly curved thin or thick shell, reduced integration, hourglass control, finite membrane strains). Elastic properties of the FRP sheets are specified in Abaqus by "LAMINA" material type, which allows correlating the longitudinal and transverse elastic modulus E_1, E_2, the rigidity modulus G_{12},G_{13},G_{23}, and the Poisson coefficient N_{u12}. In the case of unidirectional fibers, it is possible to only specify E_1 and assign very small values to the other elastic properties so that the system is not affected by interaction with the other directions.
Ultimate conditions for the FRP jackets were defined by the maximum unidirectional tensile stress of the fibers f_{ju} obtained evaluating the ultimate hoop tensile strain $\varepsilon_{h,rup}$ according to Lim and Ozbakkaloglu (2015):

$$f_{ju} = E_j \cdot \varepsilon_{h,rup} \quad (2a)$$

$$\varepsilon_{h,rup} = (0.9 - 2.3 \cdot f_{c0} \cdot 10^{-3} - 0.75 \cdot E_j \cdot 10^{-6}) \cdot \varepsilon_{ju} \quad (2b)$$

in which E_j and ε_{ju} are the elastic modulus and the ultimate tensile strain of the fibers respectively.

Concrete Damaged Plasticity Model (CDPM) was used to reproduce the compressive behavior of FRP-confined concrete. Formulations defining the behavior of concrete under multi-axial stresses include the *damage variable*, the *yield criterion*, the *flow rule* and the *hardening/softening* rule that define the non-linear behavior of concrete. The *yield criterion* described in Lubliner et al. (1989) and modified in Lee and Fenves (1998) sets out the

yielding conditions when concrete is under multi-axial compression. The *flow rule* determines the direction of the plastic deformations and describes the relationship of plastic lateral strain and plastic axial strain increments, assuming a *non-associated potential plastic flow*. The above formulations can be managed in Abaqus (Theory and User manuals 2013) by the users defining the *plasticity parameters.* These are the dilation angle ψ, the ratio of the compressive strength under biaxial loading and uni-axial compressive strength f_{b0}/f_{c0}, the flow potential eccentricity e, the viscosity parameter μ and the ratio K_c of the second stress invariant on the tensile meridian and that on the compressive meridian for the yield function.
In this work the plasticity parameters were defined according to Hany et al. (2016), considering the damage parameter dc=0 for concrete under tri-axial compression.

Preload simulation

The numerical process of compression tests for preloaded specimens was performed by means of a multistep analysis method combined with the use of the de-activation/reactivation elements technique. The assembled model was defined before the analysis assigning the properties to the materials used for the confinement in such a way to activate its contribution on the global response only when desired. Specifically, in the first step the axial force related to the preloading level index was applied to the non-confined element (with the confining device deactivated). The stress/strain state at the end of the analysis corresponded therefore to the tensional state relative to the preload level. In the second step, the confining device became active in deformed condition, characterized by the congruence of the nodal displacements, but with zero stress/strain. After the activation of the confining device the analysis was performed displacement controlled up to the failure of the composite jacket. Therefore, in terms of compressive stress-strain behavior, the concrete column provided "unconfined type" response up to the end of the preload and subsequently the compressive response changed in "confined" according to the experimental tests. Time-dependent effects were neglected in the FE model.
In Figure 4 the computational process is shown for two cases of compression tests with no preload and with preload of 85% of f_{c0} before wrapping. Compressive stress for concrete, lateral confinement pressure, axial and lateral strains of the middle section of the cylinder were evaluated during the numerical simulation for each step of analysis. In detail, in the case of preload, the first step of analysis evaluates the response of the plain concrete only up to the beginning of the second step in which the FRP jackets are activated. In fact, lateral confinement pressure returns zero values although the increasing of the axial stress, the axial and the lateral strains. During the second step of analysis the concrete is under tri-axial compression state because affected by the lateral confinement pressure. In the case of compression test with no preload, the entire numerical process was performed in the second step with the FRP jackets activated from the first stages of the analysis step.
In both cases there are no differences in terms of confined compressive strength, as the failure conditions occur only when the fibers reach the ultimate strain. For concrete compression curves characterized by strain-hardening behavior, the confined concrete strength corresponds to the lateral confinement pressure, which always reaches the same maximum value. This aspect agrees also with the ultimate conditions of the specimens tested experimentally.

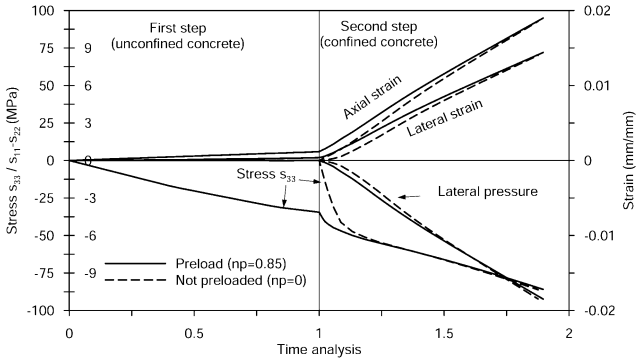

Figure 4: FE computational process for multistep analysis

RESULTS AND DISCUSSIONS

In Fig. 5 the stress and strain field in the concrete cylinder confined with FRP are shown for three significant steps of the numerical process. The end of the first step (Fig. 5 a-b) in which the unconfined concrete cylinder reached the preload without any contribution of the FRP jacket; the beginning of the second step at increment 0 (Fig. 5 c-d) in which the concrete cylinder keeps the same stress/strain configuration of the previous step and the FRP jacket becomes "active" with stress/strain but having the same shape of the cylinder; the end of the analysis (Fig. 5 e-f) represented by the reaching of the ultimate hoop strain of the jackets.
Experimental and numerical results of the ultimate conditions are reported in Table 2.

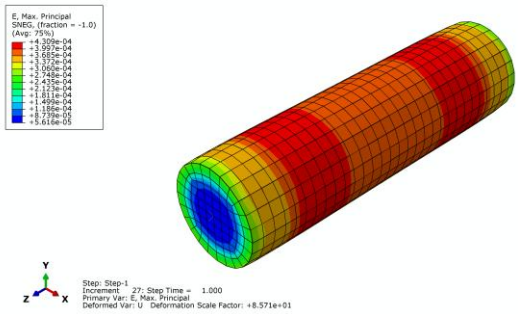

(a) Strain field at the end of the preloading

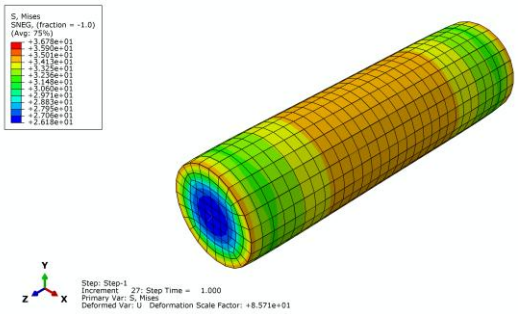

(b) Stress field at the end of the preloading

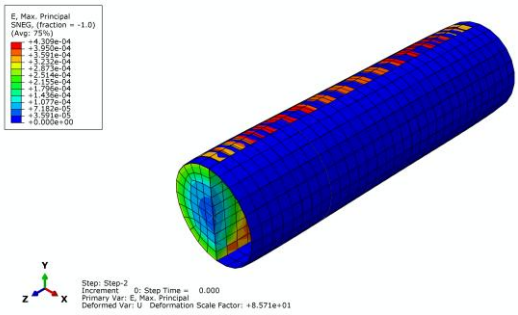

(c) Strain field at the time activation of the jacket

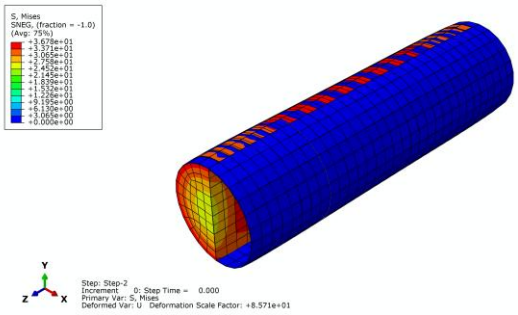

(d) Stress field at the time activation of the jacket

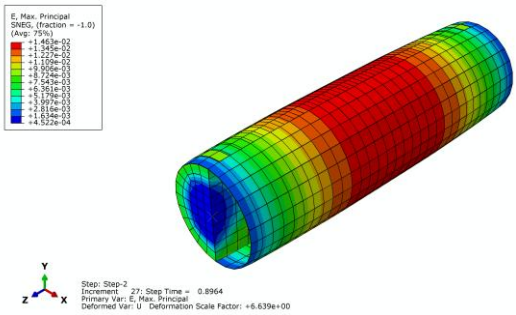

(e) Strain field at the end of the analysis

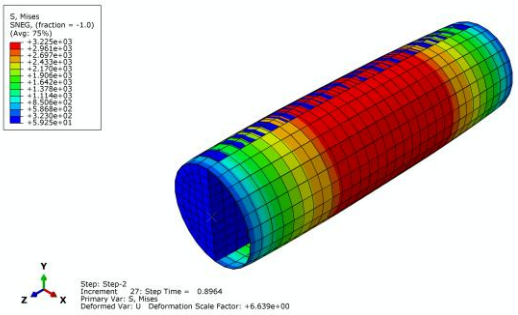

(f) Stress field at the end of the analysis

Figure 5: Stress and strain fields during the multistep analysis

Comparisons between numerical and experimental results show a good agreement confirming the reliability of the FE model in the prediction of both the compressive stress-strain response and the confined concrete strength and strain capacity. A very small reduction of the axial stress vs axial strain curve was obtained by assigning the preloading level on the plain concrete model. In details, in the case of a preloading level up to 40% f_{c0}, the effect of preloading may be neglected entirely. As long as the unconfined concrete is elastic, the response of the preloaded configuration overlaps the monotonic response. When the preloading level increases, a reduction of the axial stress vs axial strain response becomes significative.

Although the preload level in the specimens may change, the strength corresponding to the collapse after the confinement results unchanged. Also, it corresponds to the ultimate deformation of the carbon fibers. Specimens confined after different preload are able to carry the same collapse load, showing a reduction in the secant stiffness of the stress-strain law, in both experimental and numerical cases. This reduction increases with the increasing of the preload level.

Table 2: Experimental and predicted results

Specimens	f_{c0} (MPa)	E_{cm} (MPa)	n_P (%)	ε_h (%)	Experimental $f_{c,max}$ (MPa)	Experimental ε_{cu} (%)	Experimental $\varepsilon_{h,rup}$ (%)	FE Predicted f_{cu} (MPa)	FE Predicted ε_{cu} (%)	FE Predicted $\varepsilon_{h,rup}$ (%)
A1	38.13	32586	/	0.092	37.93	0.200	0.092	101.06	2.192	1.164
AS1			/	1.256	101.85	2.302	1.256			
AS2			/	/	99.28	2.262	/			
AS3			/	1.177	101.45	2.254	1.177			
AP40-1			39	/	92.22	2.163	/	101.05	2.208	1.174
AP40-2			39	1.149	99.42	2.391	1.149			
AP60-1			58.4	/	97.23	2.452	/	99.02	2.162	1.149
AP60-2			58.4	1.307	101.29	2.605	1.307			
AP80-1			78	1.219	98.61	2.639	1.219	98.75	2.174	1.157
AP80-2			78	1.130	92.89	2.547	1.130			
B1	41.7	35253	/	0.058	41.89	0.180	0.058	77.72	1.563	1.160
BS1			/	1.04	75.39	1.622	1.04			
BS2			/	1.047	78.71	1.671	1.047			
BP55-1			55	1.067	77.28	1.773	1.067	77.27	1.572	1.169
BP55-2			55	1.069	77.62	1.789	1.069			
BP70-1			71	1.043	81.29	1.740	1.043	77.40	1.589	1.183
BP70-2			71	1.056	79.11	1.622	1.056			
BP90-1			88.5	/	84.44	2.172	/	77.01	1.608	1.200
BP90-2			88.5	1.079	77.83	1.916	1.079			

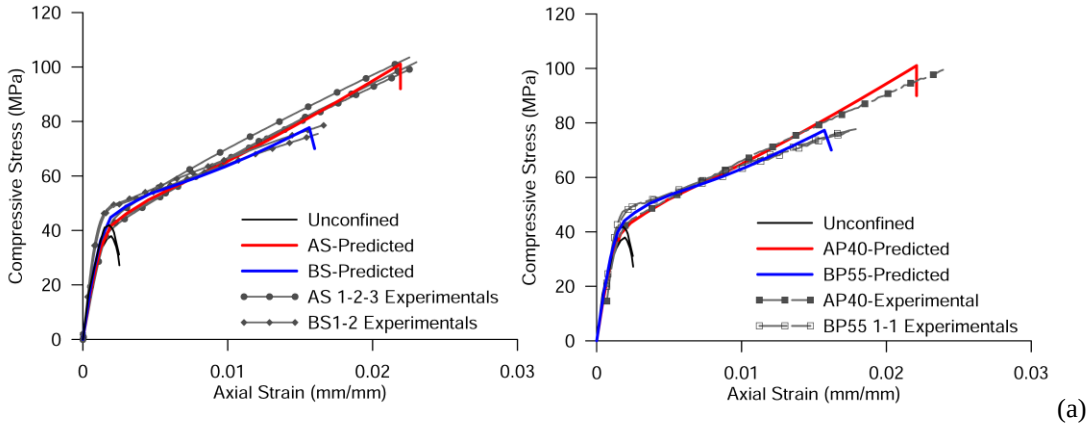

(a) Compression tests with no preload (b) Preload np=0.4 and 0.55

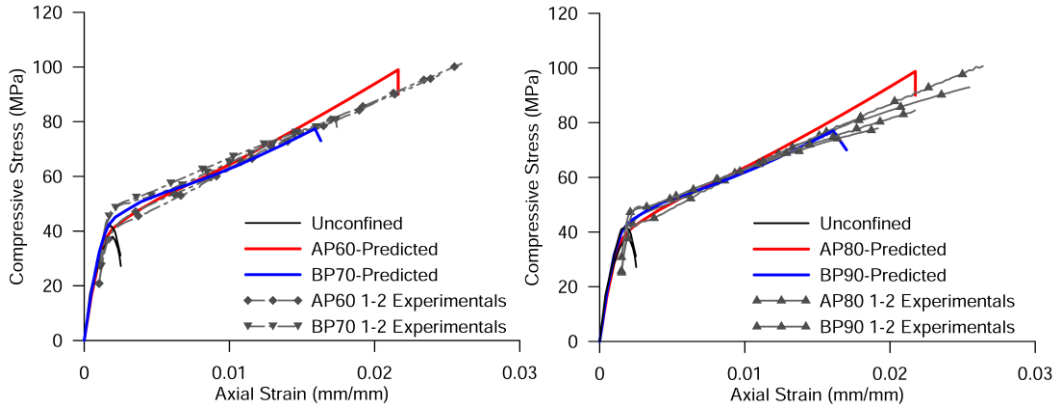

(a) Preload np=0.6 and 0.7 *(b) Preload np=0.8 and 0.9*

Figure 6: Axial compressive behavior: Comparisons between experimental data and FE model prediction

CONCLUSIONS

The present paper presented a finite element approach to model the compressive behavior of concrete cylinders confined with CFRP sheets using the Concrete Damaged Plasticity Model available in Abaqus.
By means of the advanced technique of deactivation/reactivation of the elements, it was possible to analyze the effects of the confinement in the presence of a preload, defining the entire model before the numerical analysis, applying a stress/strain state to the cylinder and activating the bandage with stress/strain but having the same shape of the cylinder. Therefore, the entire physical process was completely reproduced according to the experimental investigation in both cases of specimens with and without preload.
It was found that, for CFRP-confined cylinders, the presence of the preload does not significantly affect the response of the confined concrete in terms of strength. Specifically, in case of a high mechanical confinement ratio, which ensures strain-hardening behavior up to failure, the bearing capacity was almost unchanged. In case of preload only a reduction of the secant stiffness of the compressive stress-strain response was observed with the increasing the preload ratio because of a delay in the activation of the elastic confinement. For preloading levels up to about 40% of the unconfined concrete strength, the preloading levels did not produce differences in the response. However, exceeded this value, the differences become more significant suggesting that it would be appropriate to consider the preloading effects for a more appropriate reproduction of the compressive behavior.

ACKNOWLEDGMENTS

The present study was developed with the financial support of the Technical University of Munich, Department of Civil, Geo and Environmental Engineering.

REFERENCES

ABAQUS. ABAQUS Theory and User Manuals, version 6.13-1; 2013.

M.F Ferrotto, O. Fischer, R. Niedermeier (2017). "Experimental investigation on the compressive behavior of short-term preloaded carbon fiber reinforced polymer-confined concrete columns", *Structural Concrete*, 1-14, https://doi.org/10.1002/suco.201700072.

Z. He, P. Jin (2011). "Axial Compressive Behavior of CFRP-Confined Concrete Columns Subject to Short-Term Preloading", *Advanced Material Research*, 163-167, 3830-3837.

N.F Hany, E.G Hantouche, M.H Harajli (2016). "Finite element modeling of FRP-confined concrete using modified concrete damaged plasticity", *Engineering Structures*, 125, 1-14.

J. Lee, G.L Fenves (1988). "Plastic-Damage Model for Cyclic Loading of Concrete Structures." *Journal of Engineering Mechanics ASCE*, 124, 892-900.

J. Lubiner, J. Oliver, S. Oller, E. Oñate (1989). "A Plastic Damage Model for Concrete", *International Journal of Solid and Structures*, 25, 299-326.

L. Lam, T.G Teng (2004). "Ultimate Condition of Fiber Reinforced Polymer-Confined Concrete", *Journal of Composites for Construction ASCE*, 8, 539-548.

J.C Lim, T. Ozbakkaloglu (2015). "Lateral strain-to-axial strain relationship of confined concrete", *Journal of Structural Engineering ASCE*, 141. DOI: 10.1061/(ASCE)ST.1943-541X.0001094.

Y. Pan, L. Wan, X. Wu (2015). "Analysis-Oriented Stress-Strain Model of CFRP Confined Concrete with Preload", *Journal of Southwest Jiaotong University*, 50, 461-465. (In Chinese).

M.R Spoelstra, G. Monti (1999). "FRP-confined concrete model", *Journal of Composites for Construction ASCE*, 3, 143-150.

D. Shi, Z. He (2009). "Short-Term Axial Behavior of Preloaded Concrete Columns Strengthened with Fiber Reinforced Polymer Laminate", *Computational Structural Engineering*, 1089-1098.

J.G Teng, Y.L Huang, L. Lam, L. Ye (2007). "Theoretical model for fiber reinforced polymer-confined concrete", *Journal of Composites for Construction ASCE*, 11, 201-210.